



## NumericalAnalysis of Two fluid flow in a Vertical Channelwith Thermal Slip

Vasavi Cheruku<sup>1,\*</sup> B Ravindra Reddy<sup>2</sup>

<sup>1</sup>Department of Mathematics, Sreyas Institute of Engineering and Technology, Hyderabad, Telangana

<sup>2</sup>Department of Mathematics, JNTUH College of Engineering Hyderabad, Hyderabad, 500085, India.

\*[vasvrao@gmail.com](mailto:vasvrao@gmail.com)

3800

### ABSTRACT

In the current study, thermal slip is imposed on the left boundary under the proper boundary and interface conditions, causing a coupled nonlinear system of partial differential equations to be driven by immiscible micropolar and viscous fluid flow in a vertical channel. Runge-Kutta 6<sup>th</sup> order is being implemented in Mathematica software. To make the variations of the relevant parameters easier to grasp, the velocity, angular velocity, temperature, and diffusion profiles are examined and depicted graphically. For all potential modifications of the governing parameters, the rates of mass transfer, heat transfer, and velocity transfer are tabulated. It is observed that velocity, angular velocity, and diffusion have all been significantly impacted by the thermal slip. On both boundaries, the transfer rate is reasonably affected as well.

**Keywords:** Vertical channel, micropolar fluid, thermal slip, R-K Method.

**DOI Number:** 10.48047/NQ.2022.20.12.NQ773704

**NeuroQuantology2022;20(12): 3800-3813**

### 1. INTRODUCTION

Many distinct disciplines of science, engineering, and technology deal with the two-phase flow on a daily basis. Two-phase flows provide numerous advantages in oil and gas production, gas-liquid flow in boilers, and aerosol deposition in spray treatment, to name a few. Inkjets, clouds, fog, groundwater movement, ocean waves, and pest management are all examples of two-phase flows. Several researchers [1-3] investigated two-phase flows in various geometries. Erdinc and Yilmaz [4] investigated heat transfer in communicative channels with non-parallel walls and discovered that the heat transfer rate in convergent and divergent channels is much higher than in channels with parallel walls.

MHD research has grown in importance because of its widespread application in accelerators, liquid metal cooling systems, geothermal energy extraction, compacted beds for the chemical industry, MHD power generators, plasma investigations, boundary layer control in aerodynamics, and other fields. Asadulla et al. [5] investigated hydromagnetic flow in irregularly shaped

channels. Hosseini et al. [6] used the differential transform approach to investigate flow through non-uniform channels under the influence of a magnetic field. Hatami et al. [7] investigated how a magnetic field affected the two-phase flow between two parallel plates. Kamel et al. [8] studied the transport of a fluid-particle suspension in a tube with flexible walls by accounting for slip effects along the wall. Eldesoky et al. [9] conducted an analytical study of particle suspension in a tube with undulating walls. Chalgeri and Jeong[10] conducted an experimental study of two-phase flows in a channel with rectangular walls. Chamka and Al-Rashidi [11] investigated the flow of hydromagnetic particle suspensions along a channel analytically. The thermodiffusion and diffusion thermo impacts on convective heat and mass transport along a vertical channel filled with viscous and micropolar fluids have been described by Suresh Babu et al.[12]. Bhargava et al. [13] discovered that free convection magnetic hydrodynamics micropolar fluid between two porous vertical plates decreases with increasing Hartman number.



Now a days, many researchers are interested in the methodology involving slip conditions, and there is a high demand for thermal systems dependent on the industry. Following that, other scholars applied the partial slip boundary constraints idea with variable fluids and complicated geometries. The goal of this research, inspired by Zheng et al. [14], was to examine the combined effects of partial slip and temperature jump on the free convective flow of heat-producing and absorbing fluid via a micro-channel. Haddad et al. [15,16] provide more information on velocity slips and temperature jumps. Bs Babu[17] investigates the effects of nonuniform fluid viscosity and thermal conductivity on MHD flow and heat transmission of fluid in a vertical channel with heat source by taking thermal slip. Kemparaju et al. [18] examined heat transfer in MHD Newtonian fluid flow across a stretched sheet

in the presence of velocity and thermal slip. Hayat et al. [19] investigated MHD flow and heat transfer parameters for boundary layer flow across a permeable stretched sheet with thermal slip. Suresh Babu et al[20,21] studied the Heat and mass transport fluid flow in a vertical channel using FEM. Aziz [22] studied hydrodynamic and thermal slip flow boundary layers over a flat plate with constant heat flux boundary conditions. He concluded that as the slip parameter increases, the slip velocity increases, and the wall shear stress decreases. Manjunatha et.al[23,24] used the partial slip boundary constraints idea with various fluids and complicated geometries.

The current work focuses on the numerical solution in an immiscible flow including both micropolar and viscous fluids in a vertical channel with the influence of thermal slip based on the aforementioned criteria and the significance of thermal slip.

## 2. MATHEMATICAL FORMULATION

Consider two isothermal parallel plates, divided into two regions and placed at  $y=-h_1$  &  $y=h_2$ . Region-1 is from  $-h_1 \leq Y \leq 0$  and is filled with micropolar fluid and region-2 is from  $0 \leq Y \leq h_2$  and is filled with viscous fluid. These two zones are kept at  $T_1$  and  $T_2$ , respectively, assuming that the fluid flow has a bouncing effect and is one-dimensional, laminar, immiscible, incompressible, and constant transport property. It is assumed that the fluid motion is complete and constant. The walls are isothermal with constant concentration and satisfy relation  $T_1 > T_2, C_1 > C_2$ .

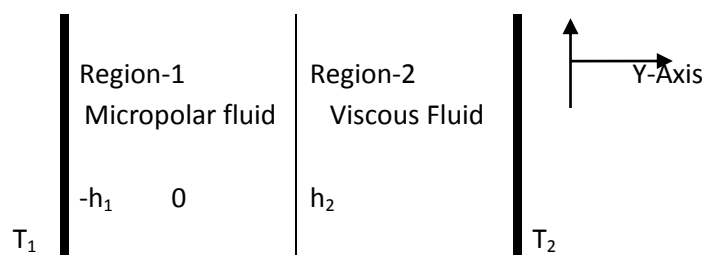


Figure-1: Schematic diagram

The following equations result from the governing equations under the presumptions mentioned above.

Region-1:



$$\frac{\partial U_1}{\partial Y} = 0 \tag{1}$$

$$\rho_1 = \rho_0[1 - \beta_{1T}(T_1 - T_0) - \beta_{1C}(C_1 - C_0)] \tag{2}$$

$$\frac{\mu_1 + K}{\rho_1} \frac{\partial^2 U_1}{\partial Y^2} + \frac{K}{\rho_1} \frac{\partial n}{\partial Y} + g\beta_{1T}(T_1 - T_0) + g\beta_{1C}(C_1 - C_0) - \frac{\sigma B_0^2 U_1}{\rho_1} = 0 \tag{3}$$

$$\gamma \frac{\partial^2 n}{\partial Y^2} - K \left[ 2n + \frac{\partial U_1}{\partial Y} \right] = 0 \tag{4}$$

where  $\gamma = \left( \mu_1 + \frac{K}{2} \right) j$

$$\frac{k_1}{\rho_1 C_p} \frac{\partial^2 T_1}{\partial Y^2} + \frac{1}{\rho_1 C_p} \left[ \mu_1 \left( \frac{\partial U_1}{\partial Y} \right)^2 + \frac{\rho_1 D_1 K_{T1}}{C_{S1}} \frac{\partial^2 C_1}{\partial Y^2} \right] = 0 \tag{5}$$

$$D_1 \frac{\partial^2 C_1}{\partial Y^2} + \frac{D_1 K_{T1}}{T_M} \frac{\partial^2 T_1}{\partial Y^2} = 0 \tag{6}$$

Region-2:

$$\frac{\partial U_2}{\partial Y} = 0 \tag{7}$$

$$\rho_2 = \rho_0[1 - \beta_{2T}(T_2 - T_0) - \beta_{2C}(C_2 - C_0)] \tag{8}$$

$$\frac{\mu_2}{\rho_2} \frac{\partial^2 U_2}{\partial Y^2} + g\beta_{2T}(T_2 - T_0) + g\beta_{2C}(C_2 - C_0) - \frac{\sigma B_0^2 U_2}{\rho_2} = 0 \tag{9}$$

$$\frac{k_2}{\rho_2 C_p} \frac{\partial^2 T_2}{\partial Y^2} + \frac{1}{\rho_2 C_p} \left[ \mu_2 \left( \frac{\partial U_2}{\partial Y} \right)^2 + \frac{\rho_2 D_2 K_{T2}}{C_{S2}} \frac{\partial^2 C_2}{\partial Y^2} \right] = 0 \tag{10}$$

$$D_2 \frac{\partial^2 C_2}{\partial Y^2} + \frac{D_2 K_{T2}}{T_M} \frac{\partial^2 T_2}{\partial Y^2} = 0 \tag{11}$$

To solve the above system of equations (1) to (11), we considered the following boundary and interface conditions.

$$U_1 = 0, \text{at } Y = -h_1, U_2 = 0, \text{at } Y = h_2, U_1(0) = U_2(0)$$

$$T_1 = T_0 + B \frac{\partial T_1}{\partial Y} \text{ at } Y = -h_1, T = T_2, \text{at } Y = h_2, T_1(0) = T_2(0),$$

$$C = C_1 \text{ at } Y = -h_1, C = C_2 \text{ at } Y = h_2, C_1(0) = C_2(0),$$

$$n = 0 \text{ at } Y = -h_1, (\mu_1 + K) \frac{\partial U_1}{\partial Y} + Kn = \mu_2 \frac{\partial U_2}{\partial Y} \text{ at } Y = 0,$$

$$\frac{\partial n}{\partial Y} = 0 \text{ at } Y = 0, k_1 \frac{\partial T_1}{\partial Y} = k_2 \frac{\partial T_2}{\partial Y} \text{ at } Y = 0, D_1 \frac{\partial C_1}{\partial Y} = D_2 \frac{\partial C_2}{\partial Y} \text{ at } Y = 0.$$

The system of equations (1) to (11) is transformed into a dimensionless form using the following non-dimensional variables:

$$y = \frac{Y}{h_1} \text{ (region-1)}, y = \frac{Y}{h_2} \text{ (region-2)}, u_1 = \frac{U_1}{U_0}, u_2 = \frac{U_2}{U_0}, \theta_1 = 1 + \beta \frac{\partial \theta_1}{\partial y} \text{ at } y = -1, \beta = \frac{B}{h_1},$$

$$C_S = \frac{C_{S1}}{C_{S2}}, K_T = \frac{K_{T1}}{K_{T2}}, D = \frac{D_1}{D_2}, h = \frac{h_1}{h_2}, m = \frac{\mu_1}{\mu_2}, \alpha = \frac{k_1}{k_2}, \rho = \frac{\rho_1}{\rho_2}, b_1 = \frac{\beta_{1T}}{\beta_{2T}}, b_2 = \frac{\beta_{1C}}{\beta_{2C}}, v = \frac{v_1}{v_2}, k = \frac{K}{h_1}.$$

The following are the dimensionless representations of the governing equations:

Region-1:

$$\frac{\partial^2 N}{\partial y^2} - \frac{2K'}{2+K'} \left( 2N + \frac{\partial u_1}{\partial y} \right) = 0 \tag{12}$$

$$(1 + k) \frac{\partial^2 u_1}{\partial y^2} + k \frac{\partial N}{\partial y} + \frac{Gr}{R} \theta_1 + \frac{Gc}{R} c_1 - Mu_1 = 0 \tag{13}$$

$$\frac{1}{Pr R} \frac{\partial^2 \theta_1}{\partial y^2} + \frac{Ec}{R} \left( \frac{\partial u_1}{\partial y} \right)^2 + \frac{Du}{R} \frac{\partial^2 c_1}{\partial y^2} = 0 \tag{14}$$

$$\frac{1}{ScR} \frac{\partial^2 c_1}{\partial y^2} + Sr \frac{\partial^2 \theta_1}{\partial y^2} = 0 \tag{15}$$

Region -2

$$\frac{\partial^2 u_2}{\partial y^2} + \frac{m}{b_1 \rho h^2} \frac{Gr}{R} \theta_2 + \frac{m}{b_2 \rho h^2} \frac{Gc}{R} c_2 - \frac{mM}{h^2} u_2 = 0 \tag{16}$$

$$\frac{\rho h}{\alpha Pr R} \frac{\partial^2 \theta_2}{\partial y^2} + \frac{\rho h Ec}{m R} \left( \frac{\partial u_2}{\partial y} \right)^2 + \frac{c_s h}{DK_T} \frac{Du}{R} \frac{\partial^2 c_2}{\partial y^2} = 0 \tag{17}$$

$$\frac{h}{D} \left( \frac{1}{ScR} \right) \frac{\partial^2 c_2}{\partial y^2} + \frac{h}{K_T D} Sr \frac{\partial^2 \theta_2}{\partial y^2} = 0 \tag{18}$$



The dimensionless boundary and interface conditions thus formed are:

$$\begin{aligned}
 u_1 = 0 \text{ at } y = -1, u_2 = 0 \text{ at } y = 1, u_1(0) = u_2(0), \\
 \theta_1 = 1 + \beta \frac{\partial \theta}{\partial y} \text{ at } y = -1, \theta_2 = 0 \text{ at } y = 1, \theta_1(0) = \theta_2(0), \\
 c_1 = 1 \text{ at } y = -1, c_2 = 0 \text{ at } y = 1, c_1(0) = c_2(0), \\
 N = 0 \text{ at } y = -1, \\
 \frac{\partial u_1}{\partial y} + \frac{K'}{1+K'} N = \frac{1}{mh(1+K')} \frac{\partial u_2}{\partial y} \text{ at } y = 0, \\
 \frac{\partial N}{\partial y} = 0 \text{ at } y = 0, \frac{\partial \theta_1}{\partial y} = \frac{1}{h\alpha} \frac{\partial \theta_2}{\partial y} \text{ at } y = 0, \\
 \frac{\partial c_1}{\partial y} = \frac{1}{hD} \frac{\partial c_2}{\partial y} \text{ at } y = 0.
 \end{aligned} \tag{19}$$

### 3. SOLUTION OF THE PROBLEM

Using the Runge-Kutta 6<sup>th</sup> order approach, a system of nonlinear equations is numerically solved. For various governing parameter values, numerical computations have been done with the effect of thermal slip. The parameters are Thermal Grashof number (Gr), Molecular Grashof number (Gc), Reynolds number (R), Magnetic field parameter (M), Material parameter (K'), Dufour number (Du), Schmidt number (Sc), Soret number (Sr) and Eckert number (Ec). Graphical representations of the governing and slip parameters effects on the dimensionless parameters velocity, temperature, and concentration are produced. The transfer rate along both the walls are studied using the following equations:

$$\begin{aligned}
 st_1 = \left[ \frac{\partial u_1}{\partial y} \right]_{y=-1}, st_2 = \left[ \frac{\partial u_2}{\partial y} \right]_{y=1}, Nu_1 = \left[ \frac{\partial \theta_1}{\partial y} \right]_{y=-1}, Nu_2 = \left[ \frac{\partial \theta_2}{\partial y} \right]_{y=1}, \\
 Sh_1 = \left[ \frac{\partial c_1}{\partial y} \right]_{y=-1}, Sh_2 = \left[ \frac{\partial c_2}{\partial y} \right]_{y=1}.
 \end{aligned}$$

### 4. RESULTS AND DISCUSSIONS

Fig-2 to Fig-6 exhibit the effect of Grashof numbers (Gr) and Molecular Grashoff number (Gc), Material parameter (k), Reynolds number (R) and thermal slip parameter (β) on velocity profiles. It is observed that as Gr, Gc increases velocity also increases substantially. The fluid velocity increases due to the enhancement of thermal and species buoyancy forces. Where as velocity is reducing as the parameters k, R, β rises. It is significant to note that applying a transverse magnetic field acts as a resistive force (Lorentz force) that acts in the opposite direction of fluid motion and resists flow, hence slowing the velocity of the fluid. As the permeability parameter k increases, it is seen that the velocity profile decreases.



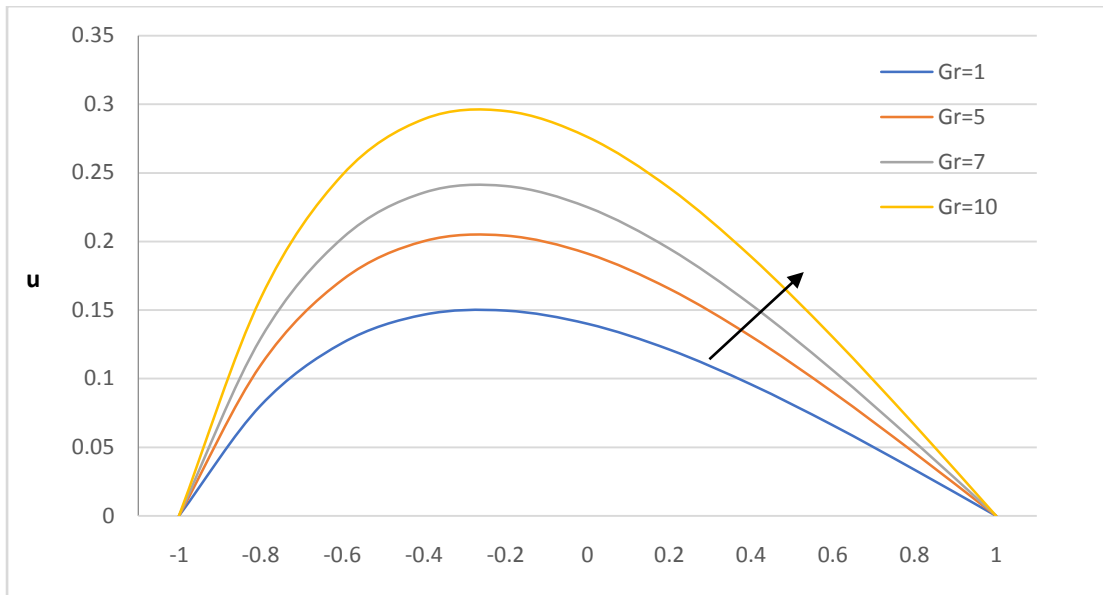


Figure-2: Variations of Velocity with Gr

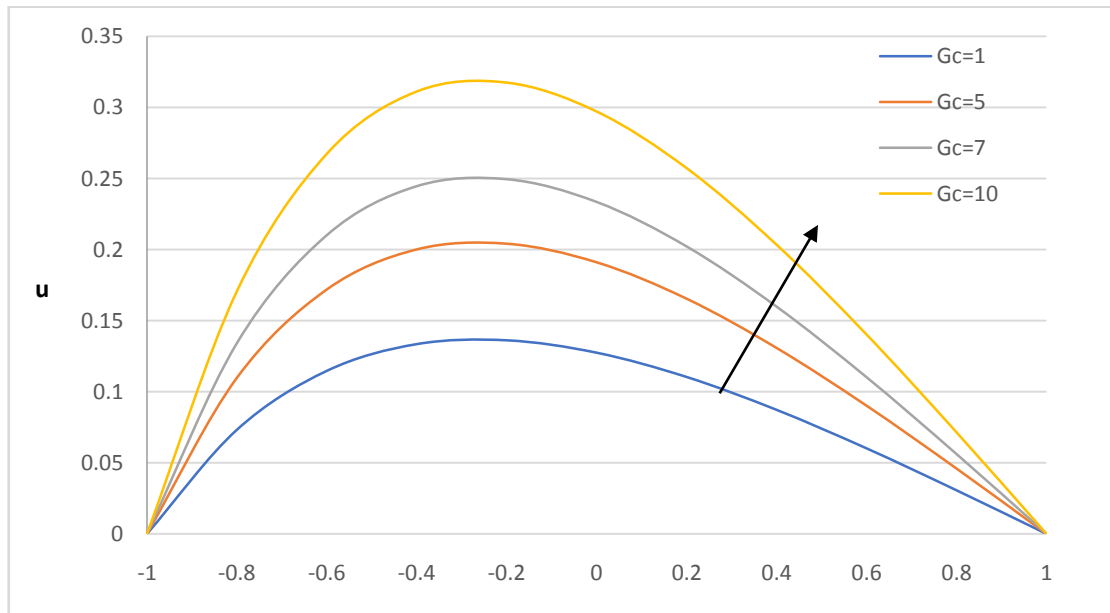


Figure 3 :Variations of Velocity with Gc

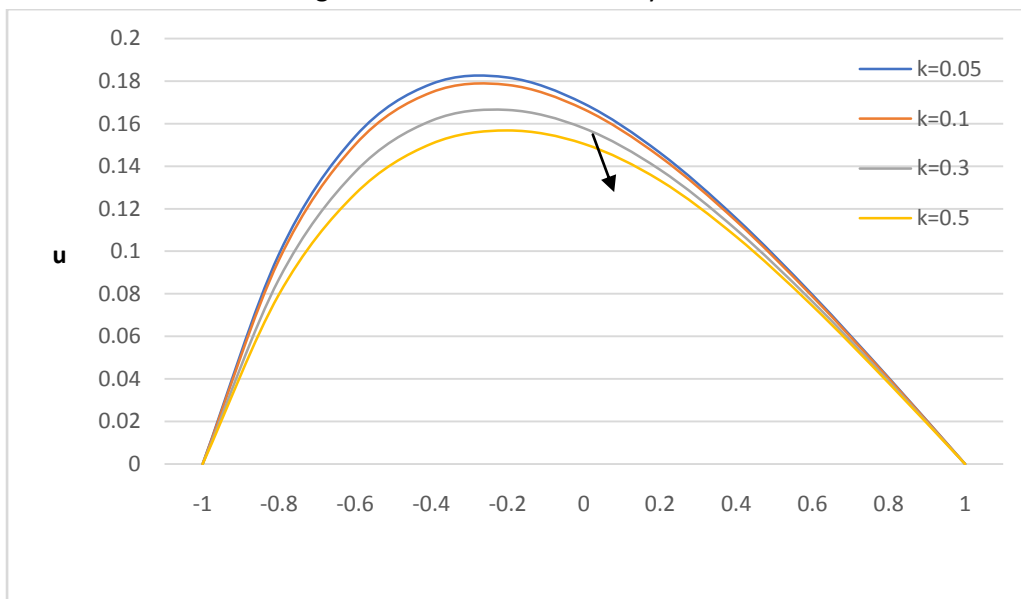


Figure 4: Variations of Velocity with k

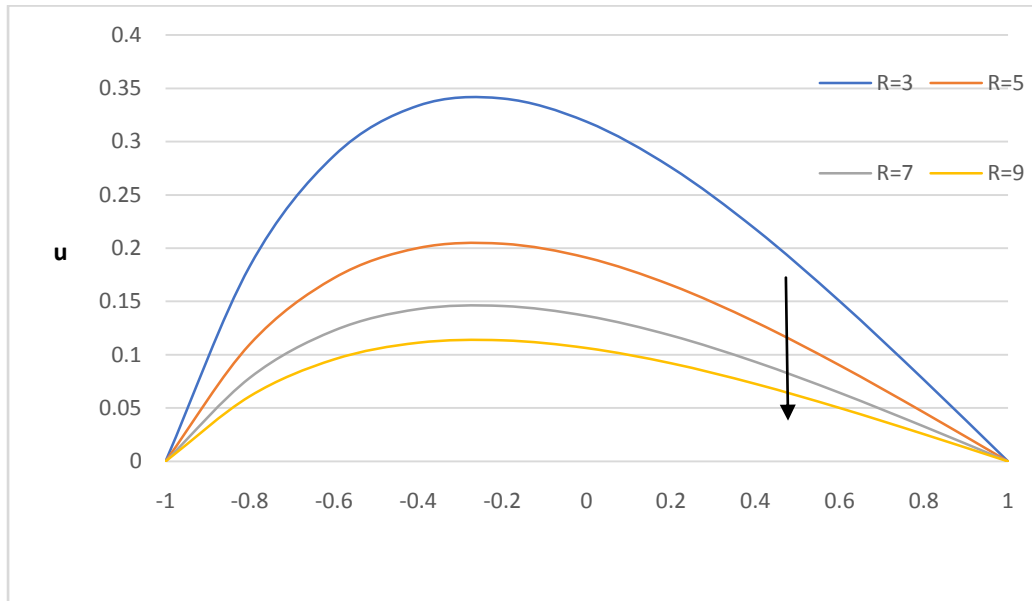


Figure 5: Variations of Velocity with R

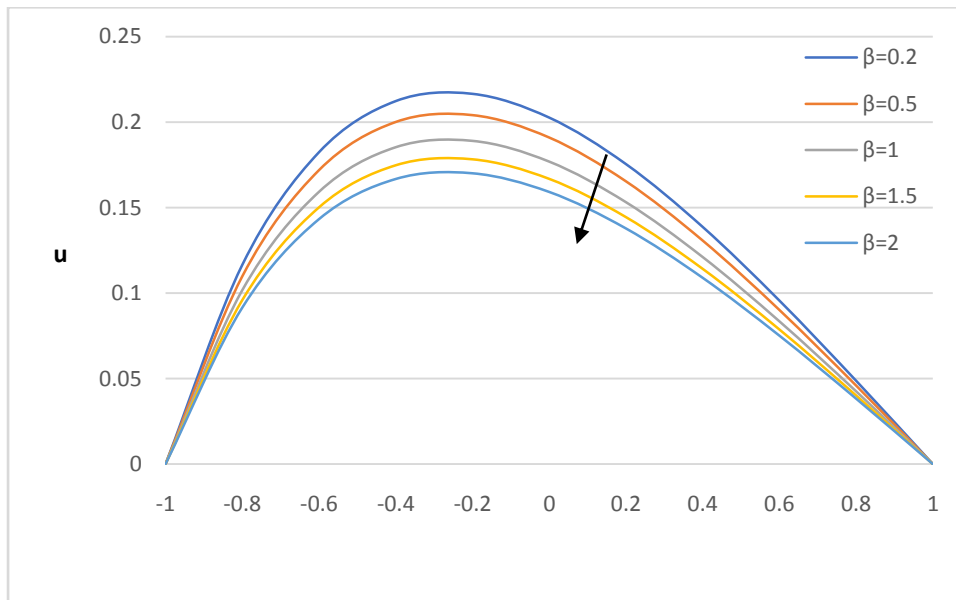


Figure 6 : Variation of Velocity with  $\beta$

Fig-7 to Fig-11 Illustrates the effect of Grashoff numbers ( $Gr$ ) and Molecular grashoff number( $Gc$ ),Material paramater ( $k$ ),Reynolds number ( $R$ )and thermal slip( $\beta$ ) on angular velocity . Angular velocity increases with an increase of  $Gr$  and  $Gc$ .An increment in the parameters  $R, k, \beta$  angular velocity is decreases substantially.



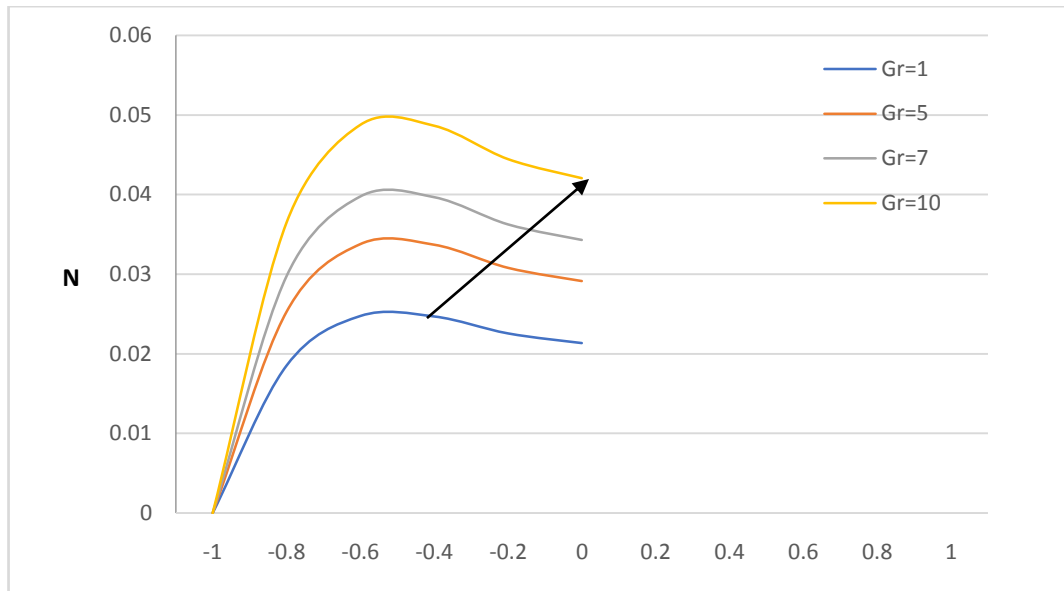


Figure 7 :Variations of Angular Velocity with Gr

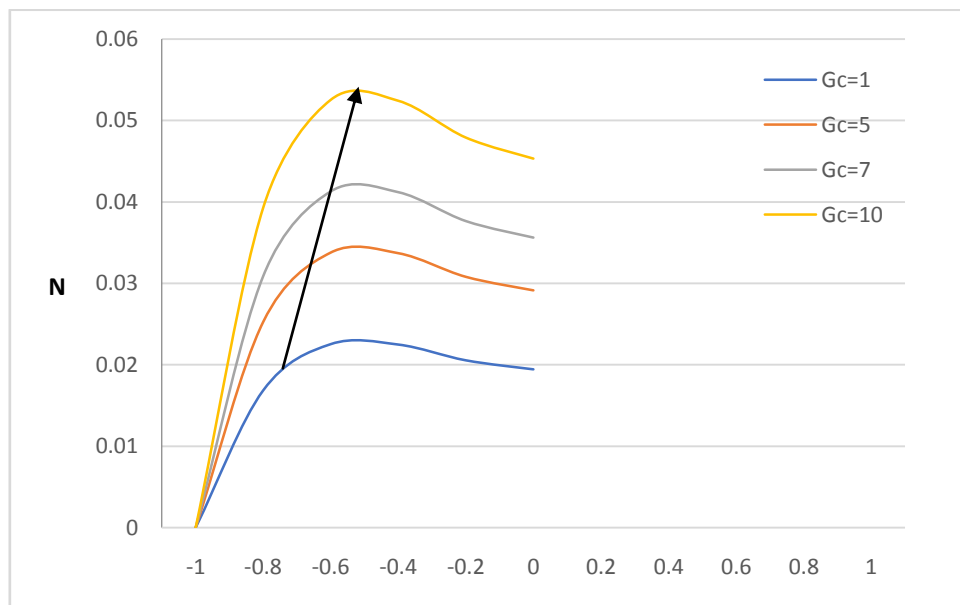


Figure 8 :Variations of Velocity with Gc



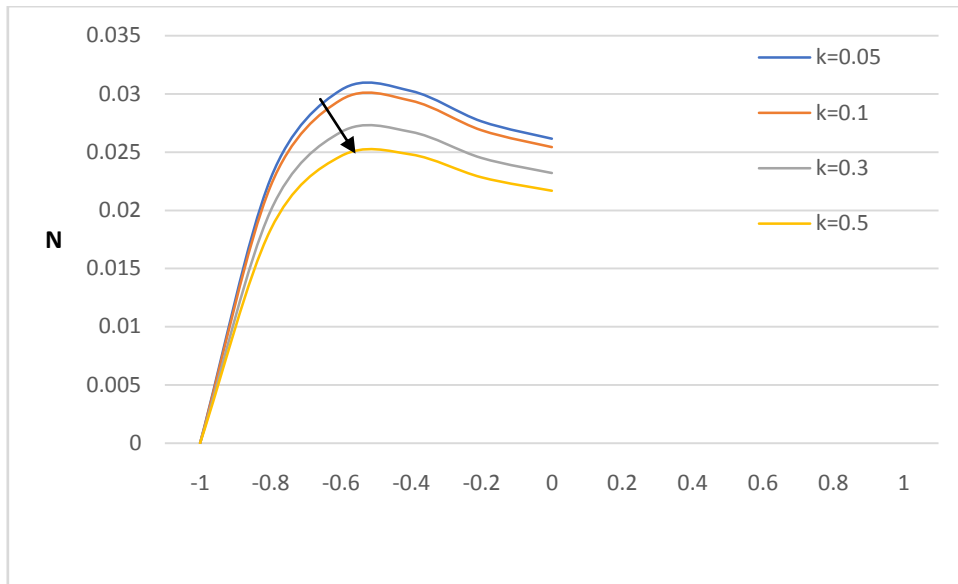


Figure 9 :Variation of Angular Velocity with k

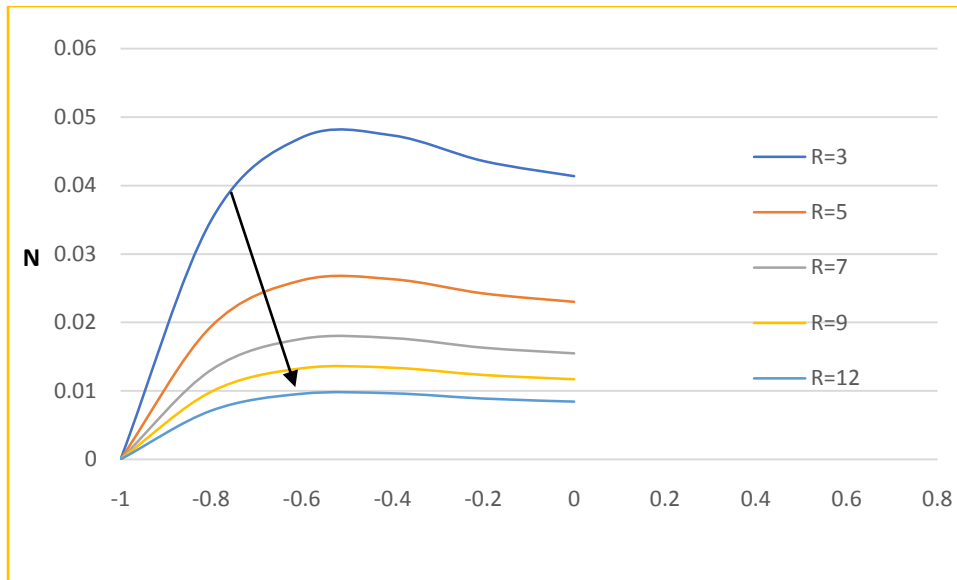


Figure 10 : Variation of angular velocity with R





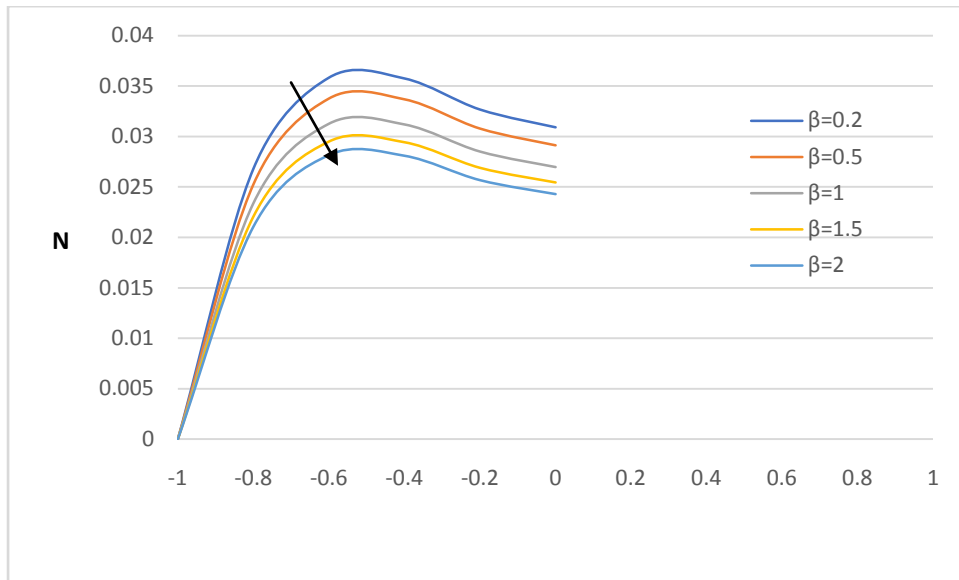


Figure 11: Variation of Angular Velocity with  $\beta$

Fig-12 to Fig-15 illustrates the influence Soret number ( $Sr$ ), Schmidt number and thermal slip ( $\beta$ ) on temperature. It is observed that there is a reduction in temperature for  $R, \beta, Sc, Sr$  increases.

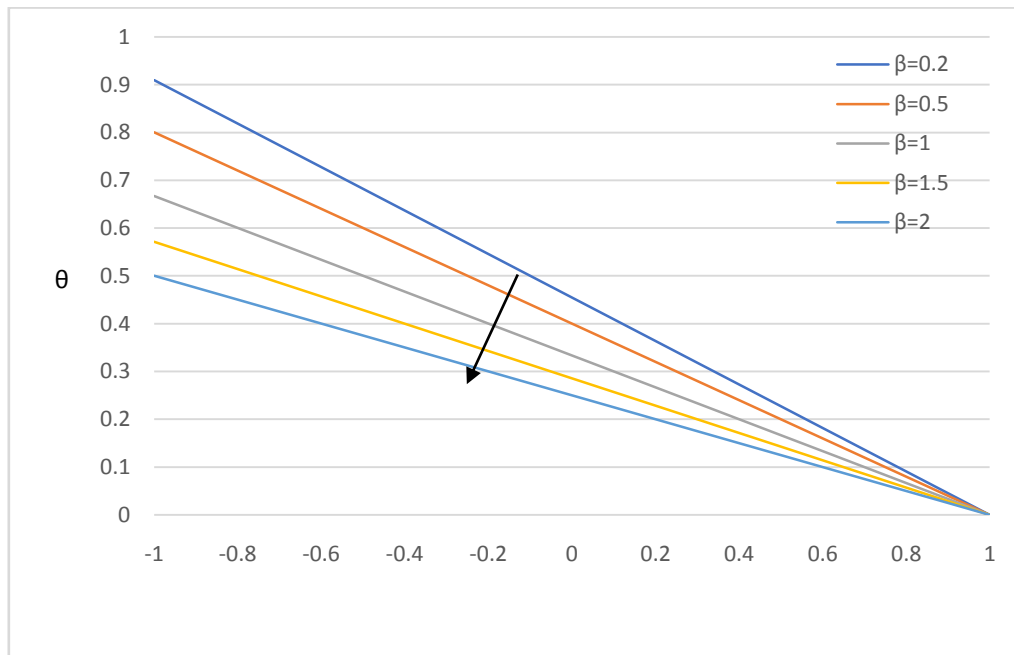


Figure 12: Variation of Temperature with  $\beta$



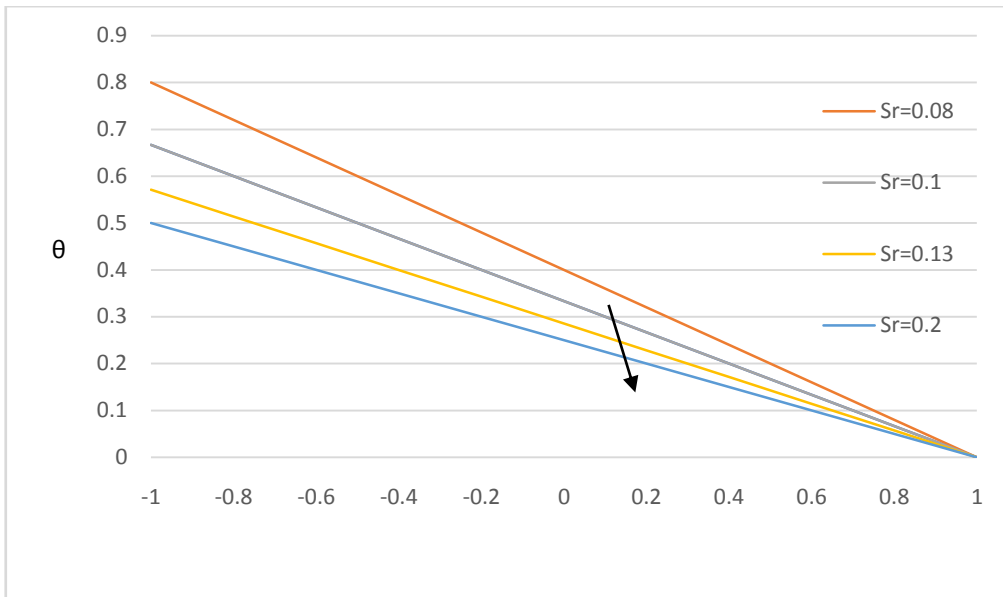


Figure 13: Variation of Temperature with Sr

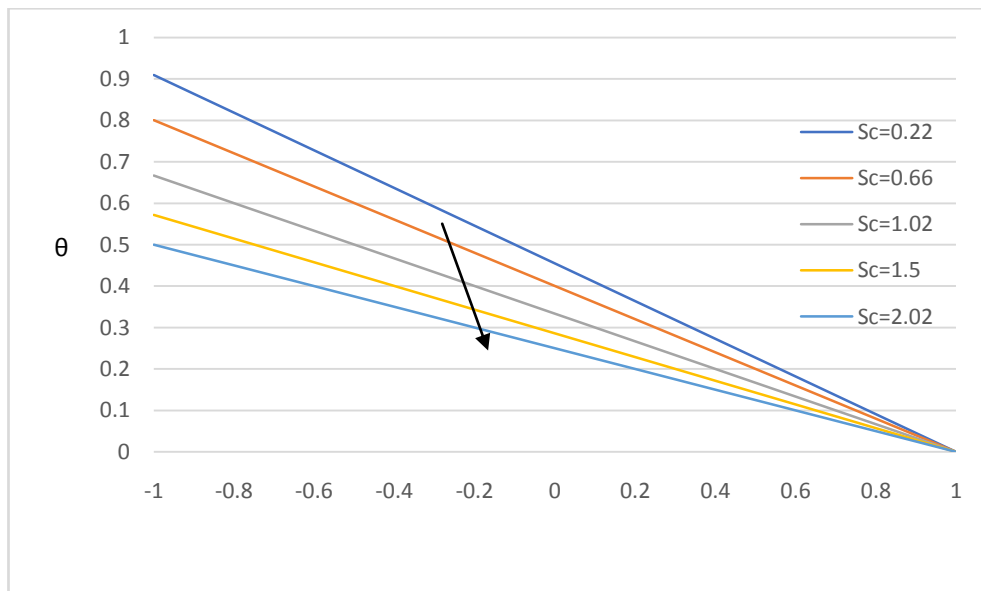


Figure 14: Variation of Temperature with Sc



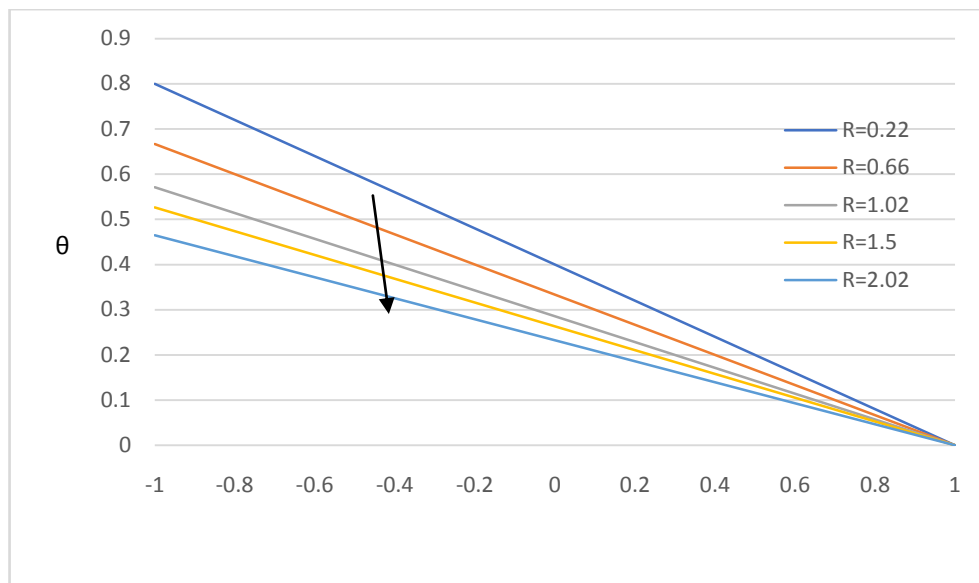


Figure 15: Variation of Temperature with R

Table 1 shows the computed shear stress, Nusselt number, and Sherwood number together with all possible impact on the governing parameters. Which are obtained when the other parameters are fixed as  $Gr=5$ ,  $Gc=5$ ,  $R=3$ ,  $M=3$ ,  $k=0.1$ ,  $Du=0.08$ ,  $Sr=0.1$ ,  $Sc=0.66$ ,  $Ec=0.001$ .

This table shows that when the buoyancy forces increase close to the borders, there is an increase in the absolute shear stress, which leads to an improvement in shearing outcomes. Shearing stress at the boundary decreases with an increase in the thermal slip, Reynolds number, magnetic field parameter, material parameter, Dufour number, Soret number, and Schmidt number.

The Nusselt number, or rate of heat transfer, decreases close to one boundary and increases at the other for the parameters  $Gr$ ,  $Gc$ ,  $Sr, Sc$ . Significant changes in the Reynolds Number are seen in the rate of heat transfer. The right plate's heat transfer rate is improved by the elevation of the inertial forces, whereas the left plates is ruined. Reversal of the effect occurs for the parameters  $M$  and  $k$ . For thermal slip parameter  $\beta$  heat transfer rate is decreased at two boundaries. The relationship between the Nusselt number and the diffusion parameters  $Du$  and  $Sr$  demonstrates that as Dufour increases, heat transfer to the left plate is enhanced and to the right boundary is reduced. For  $Sr, Sc$  it is entirely in opposition.

The Sherwood number, which measures the rate of mass transfer, increases close to the border and decreases at the other boundary for the parameters  $Gr$ ,  $Gc$ ,  $R$ ,  $Sr$ ,  $Sc$ , and  $Ec$ . Mass transfer decreases close to the left border and increases at the right boundary for the other parameters  $M$ ,  $k$ , and  $Du$ , respectively and for slip parameter rate of mass transfer is decreased at both borders.

	St-1	St-2	Nu-1	Nu-2	Sh-1	Sh-2
Gr						
2	0.511333	-0.16945	-0.399969	-0.40002	-0.50001	-0.5
5	0.697282	-0.23108	-0.399943	-0.40004	-0.50002	-0.49999
7	0.821255	-0.27216	-0.399921	-0.40006	-0.50003	-0.49999
10	1.00723	-0.3338	-0.399881	-0.40009	-0.50005	-0.49998
Gc						
2	0.464852	-0.15405	-0.399975	-0.40002	-0.50001	-0.5
5	0.697282	-0.23108	-0.399943	-0.40004	-0.50002	-0.49999



7	0.852237	-0.28243	-0.399915	-0.40006	-0.50004	-0.49999
10	1.08467	-0.35946	-0.399862	-0.4001	-0.50006	-0.49998
R						
2	1.16218	-0.38515	-0.39985	-0.40011	-0.50004	-0.49999
5	0.697282	-0.23108	-0.399943	-0.40004	-0.50002	-0.49999
7	0.498054	-0.16505	-0.399969	-0.40002	-0.50002	-0.49999
9	0.387374	-0.12837	-0.39998	-0.40002	-0.50002	-0.49999
12	0.29053	-0.09628	-0.399988	-0.40001	-0.50001	-0.5
$\beta$						
0.2	0.739536	-0.24508	-0.454473	-0.45458	-0.50003	-0.49999
0.54	0.697282	-0.23108	-0.399943	-0.40004	-0.50002	-0.49999
1	0.645637	-0.21396	-0.333293	-0.33338	-0.50002	-0.49999
1.5	0.608747	-0.20174	-0.285683	-0.28576	-0.50002	-0.49999
2	0.581078	-0.19257	-0.249975	-0.25004	-0.50002	-0.49999
k						
0.05	0.627256	-0.20335	-0.285682	-0.28576	-0.50002	-0.49999
0.1	0.608747	-0.20174	-0.285683	-0.28576	-0.50002	-0.49999
0.3	0.546076	-0.19607	-0.285689	-0.28575	-0.50002	-0.5
0.5	0.497064	-0.19144	-0.285693	-0.28574	-0.50001	-0.5
Sr						
0.05	0.497064	-0.19144	-0.285694	-0.28574	-0.50001	-0.5
0.08	0.497064	-0.19144	-0.285693	-0.28574	-0.50001	-0.5
0.1	0.497064	-0.19144	-0.285693	-0.28574	-0.50001	-0.5
0.13	0.497065	-0.19144	-0.285691	-0.28575	-0.50002	-0.49999
0.2	0.497065	-0.19144	-0.285689	-0.28575	-0.50003	-0.49999
Sc						
0.22	0.497064	-0.19144	-0.285694	-0.28574	-0.5	-0.5
0.66	0.497064	-0.19144	-0.285693	-0.28574	-0.50001	-0.5
1.02	0.497065	-0.19144	-0.285691	-0.28575	-0.50002	-0.49999
1.5	0.497065	-0.19144	-0.285688	-0.28575	-0.50003	-0.49999
2.02	0.497067	-0.19144	-0.285684	-0.28576	-0.50005	-0.49998

**Table 1:** Numerical values of shear stress, Nusselt number, Sherwood numbers

**5. CONCLUSIONS**

The impact of all governing parameters was investigated and displayed graphically. Some of the salient findings are as follows:

- Gr, Gc, R, and k have a significant impact on the velocity, angular momentum, temperature, and diffusion profiles.
- There is a significant effect of all the parameters on the rate of shear

stress, rate of heat transfer, and rate of mass transfer.

- All profiles are significantly impacted by the thermal slip that is installed on the left wall.

**REFERENCES**

[1] A.J. Chamkha, Hydromagnetic two-phase flow in a channel, Int. J. Eng. Sci. 33 (1995) 437-446.  
 [2] M.Z. Podowski, Multidimensional modeling of two-phase flow and heat



- transfer, *Int. J. Numer. Methods Heat Fluid Flow* 18 (3/4) (2008) 491-513.
- [3] S.K.R. Cher, S. Kariveti, S. Pushpavanam, Experimental and numerical investigations of two-phase (liquid-liquid) flow behavior in rectangular microchannels, *Ind. Eng. Chem. Res.* 49 (2010) 893-899.
- [4] E.M. Sparrow, R. Ruiz, L.F.A. Azevedo, Experiments and numerical investigation of natural convection in convergent vertical channels, *Int. J. Heat Mass Tran.* 31 (5) (1988) 907-915
- [5] M. Asadullah, U. Khan, N. Ahmed, R. Manzoor, S. Tauseef, MHD flow of a Jeffery fluid in converging and diverging channels, *Int. J. Mod. Math. Sci.* 6 (2) (2013) 92-106.
- [6] R. Hosseini, S. Poozesh, S. Dinarvand, MHD flow of an incompressible viscous fluid through convergent or divergent channels in presence of a high magnetic field, *J. Appl. Math.* (2012) 157067.
- [7] ] M. Hatami, KhHosseinzadeh, G. Domairry, M.T. Behnamfar, Numerical study of MHD two-phase Couette flow analysis for fluid particle suspension between moving parallel plates, *J. Taiwan Inst. Chem. Eng.* 45 (2014) 2238-e2245.
- [8] M.H. Kamel, I.M. Eldesoky, P.M. Malur, R.M. Bumandown, Slip effects on peristaltic transport of a particle-fluid suspension in a planar channel, *Appl. Bionics Biomechanics* 2015 (2015) 70357.
- [9] I.M. Eldesoky, S.I. Abdelsalam, R.M. Abumandour, M.H. Kamel, K. Vafai, Interaction between compressibility and particulate suspension on peristaltically driven flow in planar channel, *Appl. Math. Mech.* 38 (1) (2017) 137-154.
- [10] V.S. Chalgeri, J.H. Jeong, Flow patterns of vertically upward and downward air-water two-phase flow in a narrow rectangular channel, *Int. J. Heat Mass Tran.* 128 (2019) 934-953.
- [11] A.J. Chamkha, S.S. Al-Rashidi, Analytical solutions for hydromagnetic natural convection flow of a particulate suspension through is flux-isothermal channels in the presence of a heat source or sink, *Energy Convers. Manag.* 51 (4) (2010) 851-858.
- [12] Babu, B. Suresh, G. Srinivas, and G. V. P. N. Srikanth. "Finite element analysis of diffusion effects on convective heat and the mass transfer of two fluids in a vertical channel."
- [13] Bhargava R, Kumar L, Takhar HS. Numerical solution of free convection MHD micropolar fluid flow between two parallel porous vertical plates. *Int. J. Eng. Sci.* 2003; 41: 123–136.
- [14] Zheng L, Niu J, Zhang X, Gao Y. MHD flow and heat transfer over a porous shrinking surface with velocity slip and temperature jump. *Math Comput Model* 2012;56:133–44.
- [15] Haddad OM, Abuzaid MM, Al-Nimir MA. Developing free convection gas flow in a vertical open-ended microchannel filled with a porous media. *Numer Heat Transfer Part A: Appl* 2005;48:693–710
- [16] Haddad OM, Al-Nimir MA, Al-Omary J Sh. Forced convection of gaseous slip flow in a porous microchannel under local thermal non-equilibrium conditions. *Transp Porous Media* 2007;67:453–71
- [17] Kiran Kumar, G., G. Srinivas, and B. Suresh Babu. "Effects of viscosity, thermal conductivity, and heat source on MHD convective heat



- transfer in a vertical channel with thermal slip condition." *Recent Trends in Wave Mechanics and Vibrations*. Springer, Singapore, 2020. 71-86.
- [18] Kemparaju, M.C., Abel, M.C. and Nandeppanavar, M.M. (2015) Heat Transfer in MHD Flow over a Stretching Sheet with Velocity and Thermal Slip Condition. *advances in Physics Theories and Applications*, 49, 25-33
- [19] T. Hayat, M. Qasim, Mesloub. MHD Flow and Heat Transfer over Permeable Stretching Sheet with Slip Conditions, *Int. J. Numer.Methods in Fluids*, Vol.66, pp. 963-975, 2010. DOI: 10:1002/flid.2294.
- [20] Suresh Babu, B., G. Srinivas, and G. V. P. N. Srikanth. "Finite Element Study of Convective Heat and Mass Transfer of Two Fluids in a Vertical Channel of Variable Width with Soret and Dufour Effects." *Numerical Heat Transfer and Fluid Flow*. Springer, Singapore, 2019. 537-546.
- [21] Srinivas, G., and B. R. K. Reddy. "Finite element analysis of free convection flow with MHD micropolar and viscous fluids in a vertical channel with dissipative effects." *Journal of Naval Architecture and Marine Engineering* 8.1 (2011): 59-69.
- [22] A. Aziz, Hydrodynamic and thermal slip flow boundary layers over a flat plate with constant heat flux boundary condition, *Commun. Nonlinear Sci. Numer. Simul.* 15 (2010) 573–580.
- [23] Manjunatha G, Rajashekhar C, Vaidya H, Prasad KV (2019) Influence of slip and convective conditions on the peristaltic mechanism of Power law fluid through an elastic porous tube with different waveforms. *MMMS* 16:340–358
- [24] Manjunatha G, Rajashekhar C, Vaidya H, Prasad KV, Makinde OD, Viharika J (2020) Impact of variable transport properties and slip effects on MHD Jeffreyfluidflow through channel. *Arabian J Sci Eng* 45:417–428

